# Event detection in prestack migration using matched filters

Jeff. K. Beckett* and John C. Bancroft


## ABSTRACT

Given a particular statistical measure of signal-to-noise (S/N), the "matched filter" is the ideal linear filter for maximizing the S/N ratio of a signal amongst random, white noise. A matched-filter approach to prestack imaging is proposed, where "signal" is defined as a particular AVO reflection coefficient surface, and all other AVO response surfaces are considered "noise". Cross-correlation of the prestack data with the signal illuminates reflection events whose AVO response curve matches that of the signal; other reflection energy is suppressed. Matched-filter imaging of synthetic P-wave data enhances the detection of Class 2 AVO events. Preliminary tests on converted wave (P-SV) synthetic data yield superior imaging, due to noise cancellation at near offsets.


## Introduction

The chief purpose of seismic migration is to reconstruct an image of the subsurface from surface seismic data. However, situations often arise where the interpreter's ability to make a high-confidence assessment of a target area is impeded by a low S/N ratio of the data. For example, high amplitude production noise from a nearby well during survey acquisition results in an overall decrease in S/N, which is particularly detrimental to P-SV wave data. In addition, it is possible that a target in P-wave data may be a low impedance contrast, Class II AVO event and is therefore difficult to image. In such cases, matched-filter theory may be applied to prestack imaging to improve imaging.

First, an overview of P-P-wave and P-SV-wave prestack kinematics is given. Matched filter theory is then introduced, followed by a discussion of the S/N enhancement resulting from the application of the matched filter to Kirchhoff prestack migration.

## Prestack kinematics

Consider a 2D seismic survey. In Kirchhoff theory, the subsurface is assumed to be composed of scatterpoints that scatter energy from any source to all receivers. Each scatterpoint spreads energy over a particular traveltime surface defined by the double-square root (DSR) equation. The P-P wave energy traveltime surface for a scatterpoint in isotropic, constant velocity media is given by (Bancroft et al.):

$$t = \left( \frac{z_0^2 + (x+h)^2}{V_P^2} \right)^{\frac{1}{2}} + \left( \frac{z_0^2 + (x-h)^2}{V_P^2} \right)^{\frac{1}{2}}; \qquad (1)$$

and the P-S wave energy traveltime surface is given by (Bancroft et al,1998)

$$t = \left( \frac{z_0^2 + (x+h)^2}{V_P^2} \right)^{\frac{1}{2}} + \left( \frac{z_0^2 + (x-h)^2}{V_S^2} \right)^{\frac{1}{2}}, \qquad (2)$$

where $h$ is half of the source-receiver offset, $z_0$ is the depth of the scatterpoint and $x$ is the source-receiver midpoint relative to the scatterpoint. $V_p$ is the P-wave velocity and $V_s$ is the S-wave velocity. An example of a P-P is shown in Figure 1, and a P-S energy traveltime surface is shown in Figure 2.

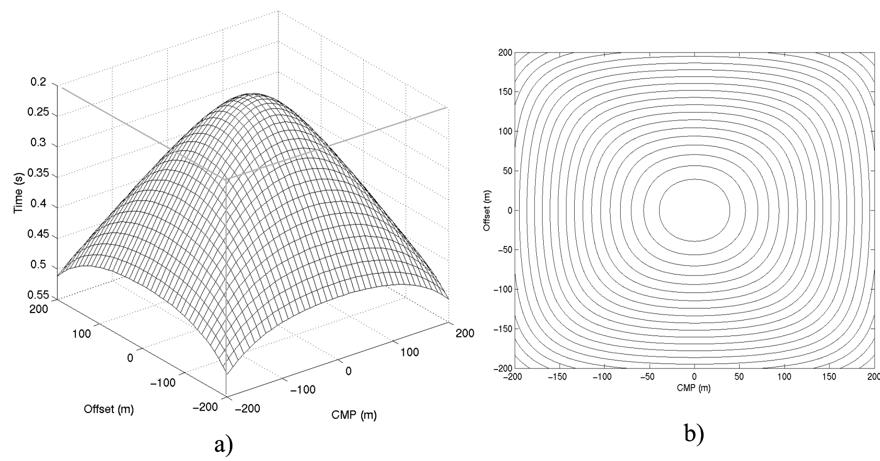


FIG. 1: a) Perspective view of a P-P wave traveltime surface for a scatterpoint located at $z_0$=100*m*. $V_P$=*800m/s.* b) plan view of (a) showing contour lines of constant traveltimes.

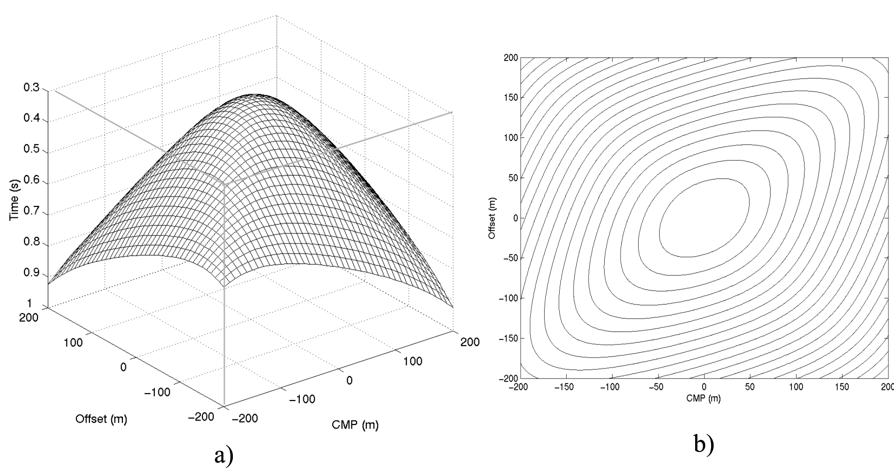


FIG. 2: a) Perspective view of a P-SV wave traveltime surface for a scatterpoint located at $z_0$=100*m*.$V_P$=*800m/s* and $V_S$=*400m/s*; b) plan view of (a) showing contour lines of constant traveltimes.

Observe that the converted wave traveltime surface differs from the P-P case in that it appears to be biased along the line $x=h$. This shape-change is due to the asymmetry of P-SV wave raypaths. Conventional Kirchhoff prestack migration involves summing over the scatterpoint-energy traveltime surface and placing the energy back at the appropriate scatterpoint location. This procedure is repeated for all scatterpoints in the prestack volume. Corrections are made to compensate for spherical divergence, obliquity ($T_0/T$), and wavelet distortion (Bancroft, 2000).

## MIGRATION

### Matched-filter theory

Assuming a known input signal in random white noise, the matched filter is designed to maximize the S/N ratio, $\mu$. Defined as the ratio of the square of signal amplitude to the square of noise amplitude, $\mu$ is given by (Lathi, 1965)

$$\mu = \frac{s_0^2(t_m)}{\overline{n_0^2(t_m)}}, \qquad (3)$$

where $s_0(t_m)$ is the output signal and $n_0(t_m)$ is the output noise at time $t_m$. The mean value of the noise is used, as the noise is random. A diagram of the matched filter shown in Figure 3, where $h(t)$ is the function of the desired optimum filter. It may be shown that $\mu$ can be maximized through selecting a filter such that (Lathi, 1965)

$$h(t) = F^{-1}\left(kS(-\omega)e^{j\omega t_m}\right), \qquad (4)$$

where $S(-\omega)$ is the Fourier transform of the time reversed input signal, $e^{-j\omega t}$ represents a time shift of $t_m$ time units, and $k$ is an arbitrary constant. Through cross-correlation of the input signal with the known impulse response, the ideal output S/N ratio is achieved. In other words, maximum event detection can be achieved when the signal, $s(t)$, is cross-correlated with the input data. It will be shown how the matched filter concept can be applied to improve event detection in prestack migration.

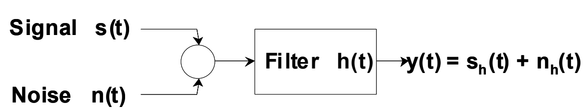


FIG. 3: Diagram of the matched filter

The proposed matched-filter migration method essentially involves cross-correlating the entire prestack volume by a Zoeppritz-defined reflection coefficient (RC) surface, which is considered signal, prior to summation. Scatterpoint energy traveltime surfaces whose AVO response matches the signal yield a greater amplitude output after migration.

A 'signal' reflection RC surface must first be defined. To justify the use of the Zoeppritz equations, each scatterpoint is assumed to be a dipping, elemental reflector of finite length. Elastic earth parameters are chosen for an arbitrary scatterpoint and its surrounding medium to yield the desired Zoeppritz-defined reflection coefficient curve as a function of incident angle. The RC curve may be viewed as a 2D surface where incident angle is a function of CMP and offset. This surface is the signal; all other possible surfaces are considered noise.

The incident angle is calculated for each sample, on a given scatterpoint energy traveltime surface within the prestack data. Each sample is then multiplied by the corresponding RC from the 'signal' surface prior to summation. This process is then repeated for all scatterpoints. Consider the P-SV example found in Figure 4, where a signal surface (top) is shown above a P-SV scatterpoint traveltime surface. Notice that this scaling function gives greater weight to input samples with greater signal content, and suppresses the input samples with greater noise content. For example, input samples on a P-S traveltime surface from a co-located source and receiver (offset=0) do not contribute any signal and are therefore given a weight of 0.

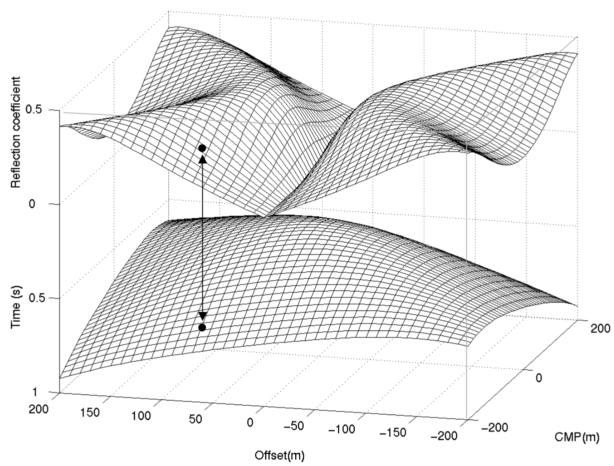


FIG. 4: A sample located on the traveltime surface (bottom) is shown to be scaled by the corresponding reflection coefficient of the signal surface (top).

## Kirchhoff EOM

The Equivalent Offset Method (EOM) of prestack time migration is computationally fast and provides excellent velocity information. This technique is based on and includes all of the benefits of Kirchhoff time prestack migration, and may be applied to both P-wave and P-S data (Bancroft et al., 1998). EOM is thus chosen for the analysis.

EOM is founded on the principles of equivalent offsets and common scatterpoint (CSP) gathers. The equivalent offset is used to enable the gathering of input samples prior to any time-shifting. Equivalent offsets are chosen such that the total traveltime from source to receiver, $t$, is equal to that of a co-located source and receiver, $2t_{e}$.

The CSP gathers are scaled, filtered to zero-phase, and corrected for normal moveout (NMO). Stacking of the CSP gather produces the output migrated trace. Note that the matched-filter amplitude-scaling occurs during the gathering process.

## P-S SYNTHETIC EXAMPLE

Synthetic P-SV prestack data were created for a single, flat reflector model using MATLAB. The model earth parameters were a chosen to incorporate a large range of RCs, and are found in Figure 5.

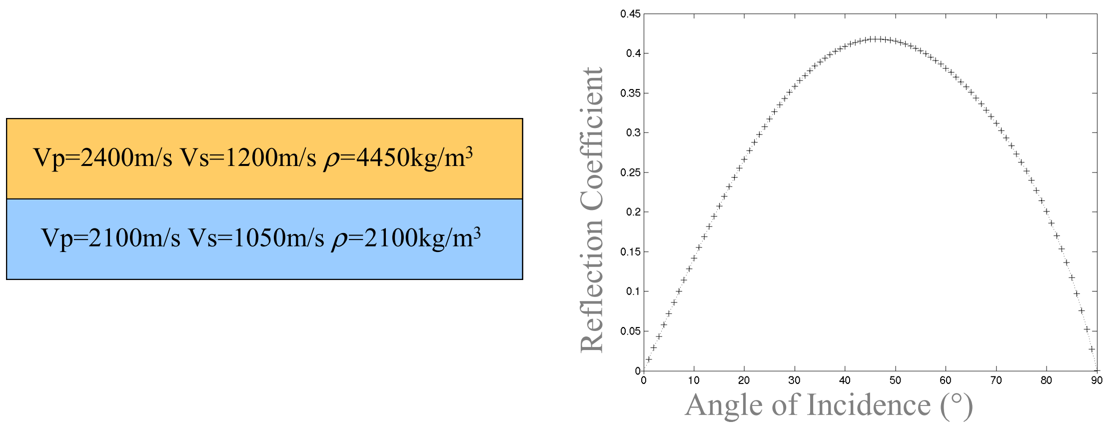


a) b)

FIG. 5: a) P-S synthetic model parameters. Depth of interface is 400m; b) Zoeppritz-defined reflection coefficient curve given the earth parameters of shown in a)

The data was acquired in a split-spread survey with a 25m shot interval, a 25m group interval, a maximum offset of 1250m, and a 2ms sample rate. A 30Hz Ricker wavelet is used as the source. Noise was added to the section such that the signal to noise ratio equals 1. The RMS value of the signal on an arbitrary pilot trace is calculated and the standard deviation of the noise is given as: noise power = (signal power) / (signal to noise ratio). Polarity has also been reversed for traces with negative offsets, and the data has been scaled to compensate for geometrical spreading.

As the objective is to improve upon conventional migration in the imaging of the reflector, the elastic earth parameters chosen to produce the signal RC surface are identical to those of the interface in the model.

A conventional CSP gather located at $x$=1250m is shown in Figure 6. In order to maximize the detection of the horizontal reflector (hyperbolic event on the CSP gather), all scatterpoint energy traveltime surfaces in the data are scaled by the signal RC surface. The same CSP gather with amplitudes scaled by the matched filter is shown in Figure 7. Both gathers are dip-limited to 45°. High-amplitude noise is apparent along the dip limits of both figures as a dip-limit taper is yet to be implemented in the CSP algorithm. The chief difference between the two figures is that the amplitude-filtered gather exhibits much less relative noise, particularly at shorter equivalent offsets. This effect is due to the scaling of samples by near-zero reflection coefficient values.

A comparison of the final output migrations is shown in Figure 8. Ten *non*-match-filtered CSP gathers, were corrected for NMO, filtered to zero-phase, stacked, and displayed as the first 10 traces in Figure 8 (from left to right). The same process was repeated for the ten match-filtered gathers, and the migrated traces constitute the remaining ten traces in the figure. Notice that the match filter has succeeded in increasing the S/N ratio, and thus imaging, of the output migration.

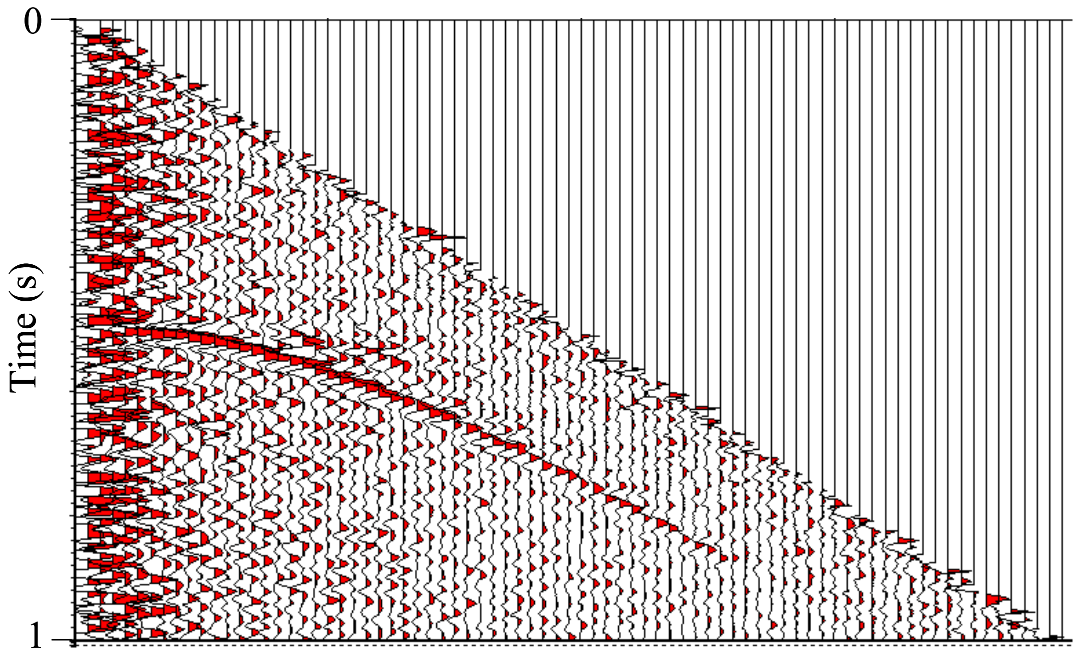


FIG. 6: Conventional CSP gather located at *x*=1250m. Equivalent offset shown on *x*-axis, where *dx*=12.5m.

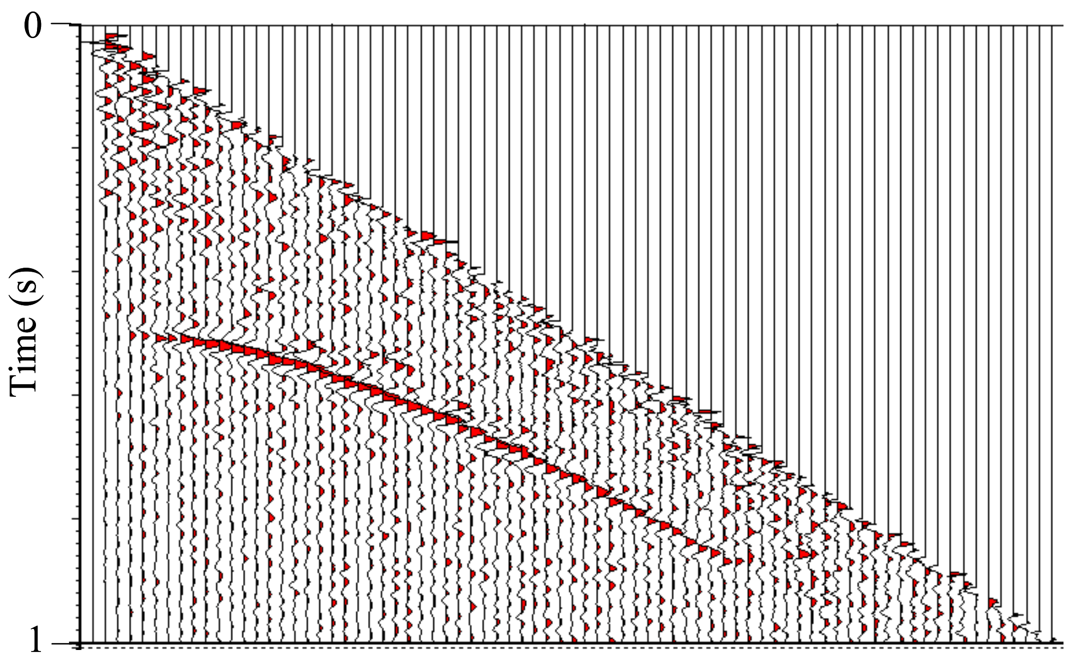


FIG. 7: CSP gather located at *x*=1250m. Amplitudes scaled by match-filtering. Equivalent offset shown on *x*-axis, where *dx*=12.5m.

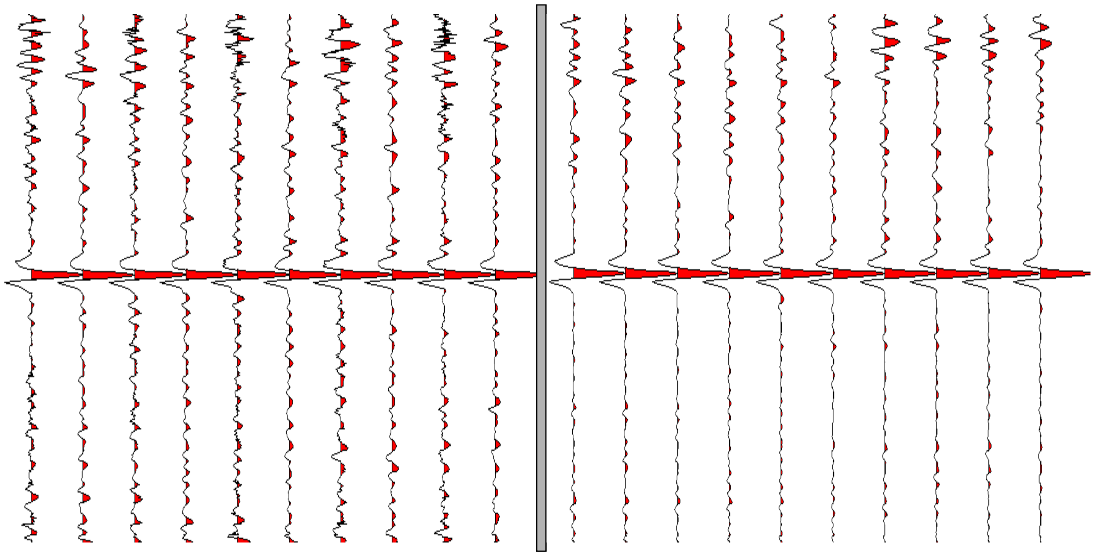

FIG. 8: The ten left-most traces are migrated CSP gathers without matched filtering. The remaining 10 traces are migrated CSP gathers located at the same positions, but have been match-filtered by a signal RC surface produced from the earth parameters found in Figure

## P-P SYNTHETIC EXAMPLE

In the previous example it has been shown that the matched filter can be applied to improve the S/N ratio in prestack migration. Using conventional P-wave synthetic data, matched filtering can also illuminate events relative to other events, as well as suppress noise.

Consider the four-layer model as shown in Figure 9. The first and third interfaces represent low-impedance contrast, Class II AVO anomalies that are not easily detected using conventional migration techniques. The second interface represents a high impedance contrast interface, e.g. an oil/water contact.

Prestack data was created for this model using the same acquisition parameters as in the converted-wave model. Two hundred metres separate each interface. Random noise was added to the prestack data.

Shown in Figure 10 are the resulting traces of two different migrations. Five output traces from a conventional migration without any matched filtering are shown on the left. Interface B is imaged well. The RC curves of interfaces A and C change polarity at mid-offsets; therefore the events tend to stack-out during migration. The five traces on the right are the migration output resulting from match-filtering the data with the signal RC surface defined by interface A. Notice the significant improvement in event detection of the first interface using the matched-filter amplitude weighting.

The signal RC curve changes polarity at mid-offsets. After match-filtering, the effective RC curve of interface B exhibits a polarity change; however the RC curve for event A becomes chiefly positive. This application of matched filtering results in the tendency for conventional high-impedance contrast events to *stack out,* and Class II AVO events to *stack in.* The detection of interface C has also improved using the 1st interface scaling, since the shape of the RC curve for interface C closely matches the signal. They essentially differ only in polarity.

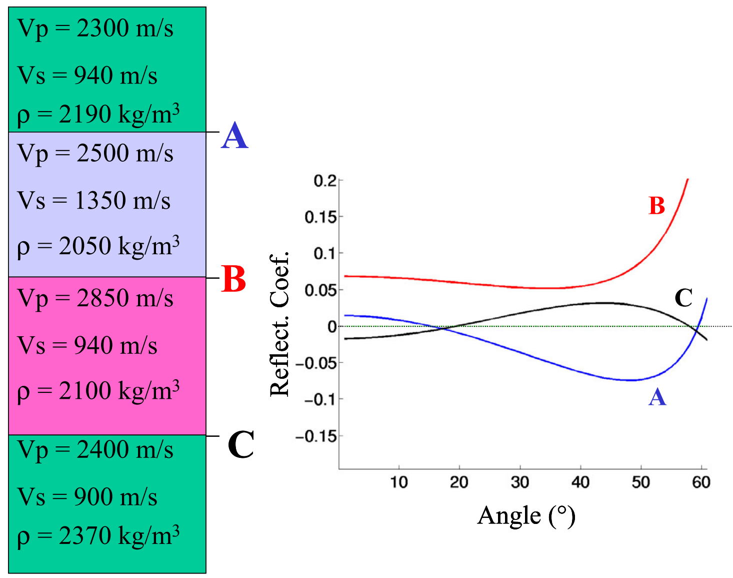


FIG. 9: Earth model for P-wave synthetic on the left. Interfaces A and C represent low impedance contrast, Class II AVO anomalies. Interface B has a high-impedance contrast and is easily imaged. Zoeppritz reflection coefficients for each interface are plotted on the right.

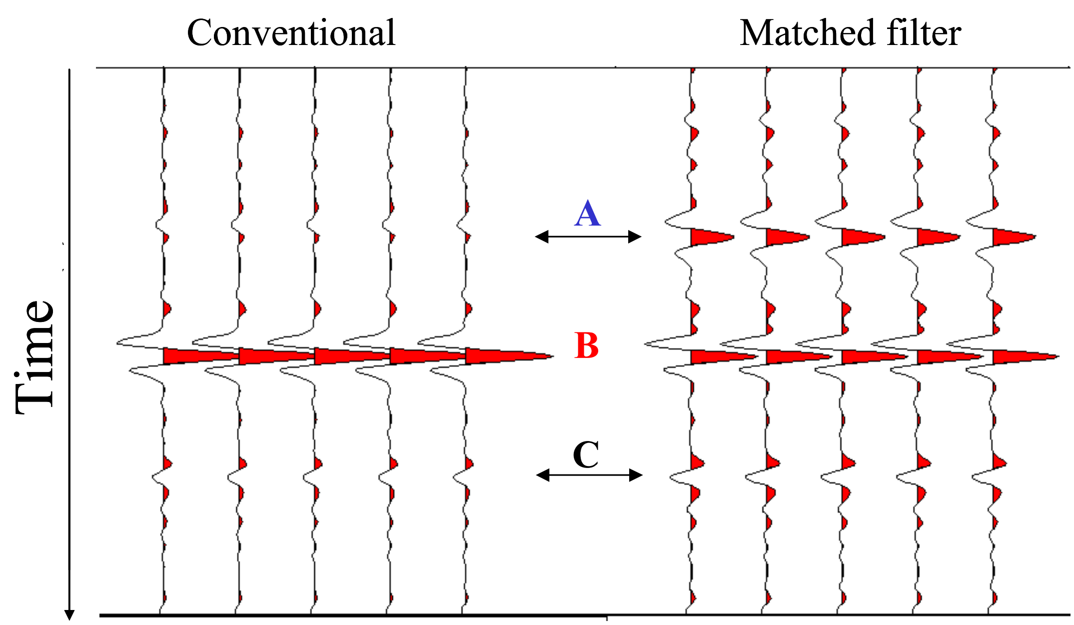


FIG. 10: Output traces from conventional prestack migration (left) compared with output-migrated traces where the amplitudes have been match-filtered to the reflection coefficients defined by the first interface.

## CONCLUSIONS

Preliminary analysis of synthetic data demonstrates the effectiveness of the matched filter in prestack imaging. A general increase in S/N is observed in P-SV data due to noise suppression at near offsets. The matched filter also shows promise as a Class II AVO anomaly indicator for P-wave data.

## REFERENCES

Bancroft, J.C., Geiger, H.D., and Margrave, G.F., 1998, The equivalent offset method of prestack time migration: Geophysics, **63**, 2042-2053

Bancroft, J.C., 2000, A practical understanding of pre- and post-stack migrations, Course Notes Series, SEG publication

Lathi, B.P., 1965, Communication Systems, John Wiley & Sons

Robinson, E.A. and Treitel,.S.,1980, Geophysical Signal Analysis, Prentice-Hall, Inc

Wang, S., Bancroft, J.C., and Lawton, D.C., 1996, Converted-wave (P-SV) prestack migration and migration velocity analysis, 66$^{th}$ Ann. Internat. Mtg: Soc. Of Expl. Geophys., 1575-1578.